Vol. 40 (2009) ACTA PHYSICA POLONICA B No 4

OVERVIEW OF EVENT-BY-EVENT FLUCTUATIONS*

Stanisław Mrówczyński

Institute of Physics, Jan Kochanowski University
Świętokrzyska 15, 25-406 Kielce, Poland
and
Andrzej Sołtan Institute for Nuclear Studies
Hoża 69, 00-681 Warsaw, Poland

(Received February 18, 2009)

Overview of event-by-event studies on relativistic heavy-ion collisions is given. I focus on fluctuation measurements and on theoretical ideas which appeared experimentally fruitful.

PACS numbers: 25.75.–q, 25.75.Gz

1. Introduction

With the advent of large acceptance detectors it became possible to observe not one but tens or even hundreds of particles produced in a single collision of relativistic nuclei. Such a multi-particle state constitutes an *event* corresponding to a single high-energy collision. Event-by-event analysis is potentially a powerful technique to study relativistic heavy-ion collisions, as magnitude of fluctuations of various quantities around their mean values is controlled by system's dynamics. For example, the energy and multiplicity fluctuations of many body system are related to, respectively, the system's heat capacity and compressibility. The two susceptibilities strongly depend the system's state and they experience dramatic changes at phase transitions. So, measuring the fluctuations we can learn about effective degrees of freedom of the system and their interactions.

Since the early 1990s the event-by-event physics has grown to a broad field of active research of relativistic heavy-ion collisions, see the review articles [1, 2]. In the following I overview the achievements and failures; I discuss difficulties and future perspectives of the event-by-event physics. I mostly present experimental results and I focus on the theoretical ideas

* Presented at the IV Workshop on Particle Correlations and Femtoscopy, Kraków, Poland, September 11–14, 2008.

which appeared to be experimentally fruitful. Although I have tried to cover the whole field, the choice of the results to be discussed is to some extend subjective.

2. Early days motivation

The first attractive idea of event-by-event analysis was formulated by Reinhardt Stock [3] who suggested to look for 'interesting' classes of events. The interesting events were meant the collisions where the quark–gluon plasma is produced or the collisions of exceptionally high multiplicity or energy density *etc.* Imagine there are 'hot' events with the temperature significantly higher than the average one. Let us further assume the event temperature can be quantified by $M(p_{\rm T})$ which is the transverse momentum averaged over particles from a given event. It is defined as

$$M(p_{\rm T}) \equiv \frac{1}{N} \sum_{i=1}^{N} p_{\rm T}^i \,, \tag{1}$$

where N is the event's multiplicity. If the 'hot' events indeed exist, then the distribution of $M(p_{\rm T})$ should reveal it. Figure 1 shows a typical example of the distribution of $M(p_{\rm T})$. The measurement was performed in central Pb–Pb collisions at 158 A GeV by NA49 Collaboration at CERN SPS [4]. As seen, no 'hot' events are observed — the $M(p_{\rm T})$ distribution is of boring Gaussian shape.

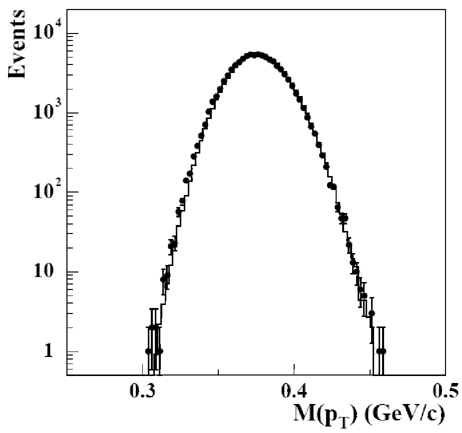

Fig. 1. The distribution of transverse momentum $M(p_{\rm T})$ measured in central Pb–Pb collisions at 158 A GeV by NA49 Collaboration. The histogram and points correspond to, respectively, the mixed and real events. The figure is taken from [4].

Figure 1 shows another typical feature of event-by-event distributions. Namely, the distribution of $M(p_{\rm T})$ obtained for the so-called 'mixed' events, where every particle is taken from a different event, is nearly identical with that obtained for real events. Since there are no inter-particle correlations in mixed events by construction, the similarity of the two distributions presented in Fig. 1 shows that particles in real events are mostly independent from each other. The same is suggested by the Gaussian shape of the distribution. The fluctuations present in mixed events are called *statistical* and the fluctuations, which remain after the statistical fluctuations are subtracted, are called *dynamical*.

Since potentially interesting information encoded in dynamical fluctuations is not easily seen in the event-by-event distributions we have to use more subtle methods to infer it. So, in the two next sections I discuss quantities to be measured.

3. Measurable quantities

In thermodynamics we have extensive quantities such as energy or particle multiplicity, which are proportional to the system's volume, and intensive quantities such as temperature or various densities, which are independent to the system's size. One is tempted to introduce analogous quantities in event-by-event physics of relativistic heavy-ion collisions. The number of participants is a natural measure of the size of system which emerges in heavy-ion collisions. Then, the quantities like the energy carried by all produced particles or particle multiplicity are approximately proportional to the number of participants and thus they are extensive.

Figure 2 shows the distribution of multiplicity of charged particles produced in Pb–Pb collisions at 158 A GeV at different centralities. The measurement was performed by WA98 Collaboration at CERN SPS [5]. The collision centrality is defined as a percentage of total inelastic cross-section $\sigma^{\rm inel}$ of nucleus–nucleus collision. The centrality of $n\%$ corresponds, roughly speaking, to the collisions with impact parameters from such an interval $[0, b]$ that πb^2 is $n\%$ of $\sigma^{\rm inel}$. As seen in Fig. 2, the smaller centrality (more central collisions), the higher average multiplicity and the smaller width of the distribution. The most upper curve corresponds to the minimum bias events when the collisions are collected with no selection — there is no centrality trigger condition. Figure 2 shows that measurements of extensive quantity like multiplicity are not very informative, as the results crucially depend on a trigger condition.

The quantities like $M(p_{\rm T})$ are expected to be analogous to thermodynamic intensive quantities. Figure 3 shows the distribution of transverse momentum $M(p_{\rm T})$ measured in central Au–Au collisions at $\sqrt{s_{\rm NN}} = 130$ GeV

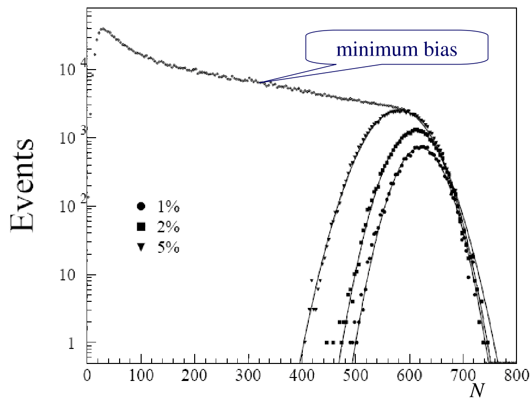

Fig. 2. The multiplicity distribution measured in Pb–Pb collisions at 158 A GeV by WA98 Collaboration. The minimum bias data and three classes of central events are shown. The figure is taken from [5].

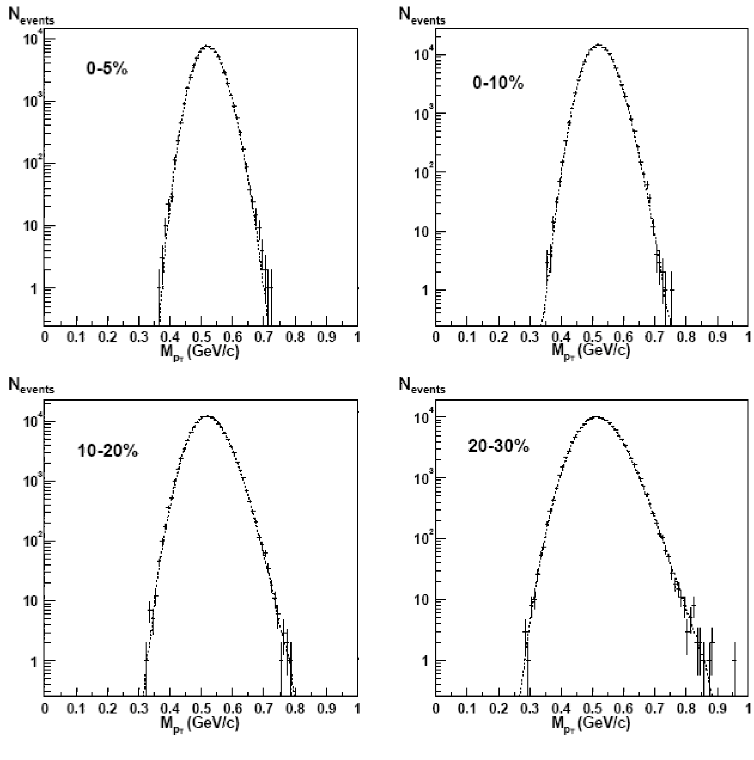

Fig. 3. The distribution of transverse momentum $M(p_{\mathrm{T}})$ measured in four centrality classes of Au–Au collisions at $\sqrt{s_{\mathrm{NN}}}$ = 130 GeV by PHENIX Collaboration at RHIC. The figure is taken from [6].

by PHENIX Collaboration at RHIC [6]. As seen in Fig. 3, the average value of $M(p_{\rm T})$ is indeed approximately independent of the system's size (centrality) but the width of the $M(p_{\rm T})$ distribution clearly depends on the system's size. And it is unclear whether the width simply depends on the trigger condition or it results from dynamics of nuclear collisions.

4. Fluctuation measures

In light of previous considerations it is desirable to construct a fluctuation measure which is truly intensive and it vanishes in absence of inter-particle correlations. Several quantities, which satisfy these conditions, have been proposed but I focus on the measure Φ introduced in [7]. It is constructed as follows. One defines the single-particle variable $z \equiv x - \overline{x}$ with the overline denoting averaging over a single particle inclusive distribution which is performed as

$$\overline{x} = \frac{1}{N_{\rm total}} \sum_{k=1}^{\mathcal{N}} \sum_{i=1}^{N_k} x_i \,, \tag{2}$$

where N_k is the particle multiplicity in k-th event, $\mathcal{N}$ is the number of events and $N_{\rm total}$ is the total number of particles in $\mathcal{N}$ events. Thus, we sum over events and over particles from every event. The event variable Z, which is a multiparticle analog of z, is defined as

$$Z \equiv \sum_{i=1}^{N} (x_i - \overline{x}) \,, \tag{3}$$

where the sum runs over particles from a given event. The averaging over events is

$$\langle Z \rangle = \frac{1}{\mathcal{N}} \sum_{k=1}^{\mathcal{N}} Z_k \,. \tag{4}$$

One observes that by construction $\langle Z \rangle = 0$. Finally, the measure Φ is defined in the following way

$$\Phi \equiv \sqrt{\frac{\langle Z^2 \rangle}{\langle N \rangle}} - \sqrt{\overline{z^2}} \,. \tag{5}$$

The measure Φ possesses two important properties:

- when particles are independent from each other — there are no correlations among particles coming from the same event, the Φ-measure vanishes identically;

- when particles are emitted by a number of identical sources, which are independent from each other, Φ has the same value as for a single source independently of the distribution of the number of sources (Φ is strictly intensive).

Due to the first property Φ is exactly zero for mixed events. Because of the second property it is strictly independent of centrality in a broad class of models of nucleus–nucleus collisions where produced particles originate form independent sources. The models include the Wounded Nucleon Model [8] and various models where a nucleus–nucleus collision is treated as a superposition of independent nucleon–nucleon interactions. In more realistic transport models like HIJING [9], VENUS [10], UrQMD [11] or HSD [12], there is an admixture of secondary interactions which break down independence of nucleon–nucleon interactions. However, Φ is still approximately independent of centrality within these models.

As already mentioned, several other fluctuation measures were introduced. In Ref. [13], see also [14], it was proposed to use

$$\sigma^2_{\rm dyn} \equiv \big\langle (X - \langle X \rangle)^2 \big\rangle - \frac{1}{\langle N \rangle} \overline{(x - \overline{x})^2}\,, \tag{6}$$

where X is the event variable

$$X \equiv \frac{1}{N} \sum_{i=1}^{N} x_i\,. \tag{7}$$

The authors of [15] advocated the measure

$$\Sigma \equiv {\rm sgn}(\sigma^2_{\rm dyn}) \frac{\sqrt{|\sigma^2_{\rm dyn}|}}{\overline{x}}\,. \tag{8}$$

We also mention here the quantity F introduced in [16] which is defined in the following way. One obtains the scaled dispersion

$$\omega \equiv \frac{\sqrt{\langle (X - \langle X \rangle)^2 \rangle}}{\langle X \rangle} \tag{9}$$

for real events and for mixed events, and then one computes

$$F \equiv \frac{\omega_{\rm data} - \omega_{\rm mixed}}{\omega_{\rm mixed}}\,. \tag{10}$$

The fluctuation measures $\sigma^2_{\rm dyn}$, Σ and F similarly to Φ vanish in the absence of inter-particle correlations. However, none of these measures is strictly intensive as Φ is. Knowing the average multiplicity $\langle N \rangle$, the measures Φ, $\sigma^2_{\rm dyn}$, Σ and F can be approximately recalculated one into another.

5. Transverse momentum fluctuations at SPS

Transverse momentum fluctuations in nucleus–nucleus collisions at SPS energies were measured by NA49 [17] and CERES [15] Collaborations. Figure 4, which is taken from [17], shows the data on p–p, C–C, Si–Si and Pb–Pb collisions at 158 A GeV. The fluctuations are measured by means of Φ at various centralities determined by number of wounded nucleons. In Fig. 1 we can hardly see the difference between the real and mixed events, Fig. 4 clearly demonstrates presence of dynamical fluctuations and thus it proves sensitivity of the Φ-measure. The magnitude of the dynamical correlations is quite small ($\Phi \leq 8$ MeV) when compared to the dispersion of the inclusive transverse momentum distribution (the second term in the definition (5)) which varies within 200 MeV $\leq \sigma_{p_{\rm T}} \leq$ 250 MeV [17]. So, the dynamical correlation is a few percent effect.

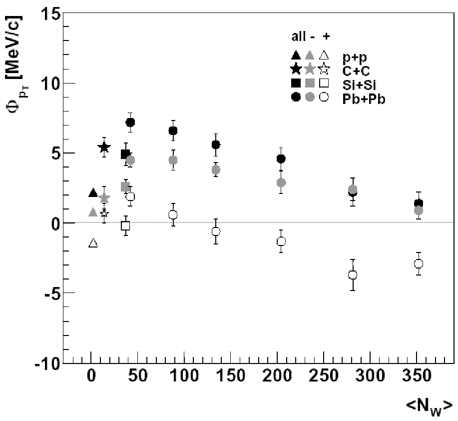

Fig. 4. $\Phi(p_{\rm T})$ as a function of wounded nucleons for nucleus–nucleus collisions at 158 A GeV. The figure is taken from [17].

We observe that the fluctuations are different for positive and negative particles. It is not surprising as the negative particles are nearly all negative pions while the positive particles include sizeable fraction of protons (the measurement shown in Fig. 4 was performed in the forward hemisphere). We also observe the centrality dependence of Φ with the maximum at rather peripheral collisions.

Although, the measure Φ is sensitive to various dynamical fluctuations, one needs more differential observables to identify a nature of the fluctuations. For such a purpose one can use the two-dimensional plot of the cumulant variables x_1, x_2 proposed in [14]. Following [18], one defines the cumulant variable

$$x(p_{\rm T}) \equiv \int_0^{p_{\rm T}} dp'_{\rm T} P(p'_{\rm T}) \,, \tag{11}$$

where $P(p_{\mathrm{T}})$ is the inclusive distribution of p_{T}. Since $P(p_{\mathrm{T}})$ is normalized to unity, $0 \le x \le 1$. And now one finds a point (x_1, x_2) for every pair of particles from the same event and constructs a two-dimensional plot such as shown in Fig. 5 [19]. In the absence of any correlations the plot is flat and various correlations generate different patterns in the plot. The example shown in Fig. 5 proves an existence of positive correlation among particles of the same p_{T} which is signaled by the ridge along the diagonal. Obviously the correlation is due to the Bose–Einstein statistics of identical pions.

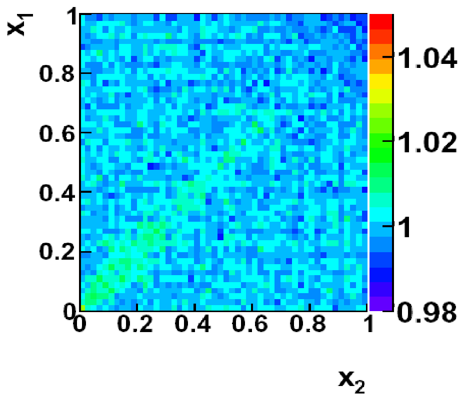

Fig. 5. Two-particle correlation plot of the cumulant variables x_1, x_2 in central Pb–Pb collisions at 158 A GeV. The figure is taken from [19].

The results of even more differential analysis performed by CERES Collaboration [20] are shown in Fig. 6. The pairs of particles, which contribute to the correlation plot, are divided into classes according to the relative azimuthal separation of the two particles $\Delta\Phi$. As seen in Fig. 6, the pattern of correlation qualitatively changes with $\Delta\Phi$. For the small separation $0^\circ < \Delta\Phi < 30^\circ$ we observe the Bose–Einstein correlation, but for the maximal separation $150^\circ < \Delta\Phi < 180^\circ$ the correlation is presumably caused by the event-by-event fluctuations of the slope of transverse momentum distribution.

The correlation plots shown in Figs. 5, 6 are indeed informative but still there is a correlation which is not clearly seen in these plots. This is the correlation of the event's transverse momentum and event's multiplicity which was observed long ago in p–p collisions at 205 GeV [21]. The correlation appears to be sufficiently strong to give a significant, if not dominant, contribution to Φ shown in Fig. 4 [22].

We conclude this section by saying that the dynamical transverse momentum fluctuations in heavy-ion collisions at SPS are of various physical origin but their total magnitude is quite small.

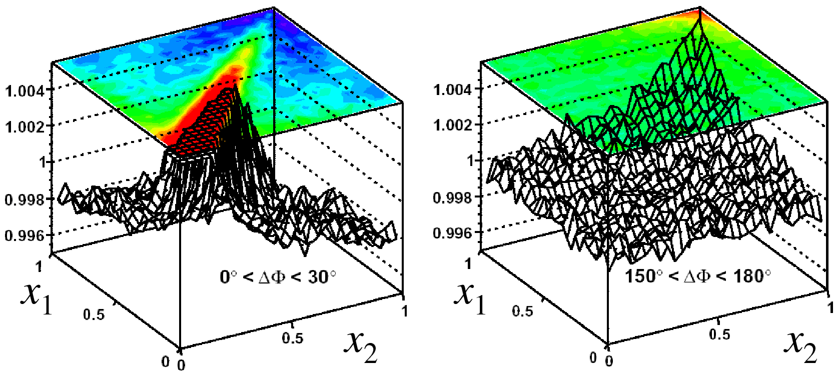

Fig. 6. Two-particle correlation plot of the cumulant variables x_1, x_2 in central Pb–Au collisions at 158 A GeV. The left and right figures, which are taken from [20], correspond to the relative azimuthal separation of the two particles $0° < \Delta\Phi < 30°$ and $150° < \Delta\Phi < 180°$, respectively.

6. Transverse momentum fluctuations at RHIC

Transverse momentum fluctuations in nucleus–nucleus collisions at RHIC were measured by PHENIX Collaboration [16] using F, see Eq. (10), and by STAR Collaboration [23] using $\sigma^2_{\rm dyn}$, see Eq. (6). Figure 7, which is taken from [16], shows the centrality dependence of $p_{\rm T}$ fluctuations which appears to be similar to that at SPS. The magnitude of the fluctuations is bigger. The measurement performed by STAR Collaboration [23], which can be easily recalculated into $\Phi(p_{\rm T})$, shows that $\Phi(p_{\rm T})$ exceeds 50 or even 70 MeV at top RHIC energy. However, it is difficult to quantitatively compare results from different experiments because the measured fluctuations depend on the acceptance which differs from experiment to experiment.

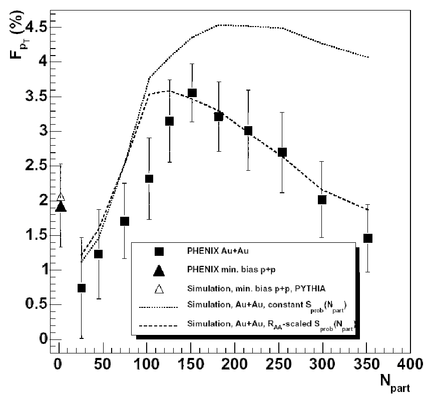

Fig. 7. $F(p_{\rm T})$ as a function of number of participating nucleons in Au–Au collisions at $\sqrt{s_{\rm NN}} = 200$ GeV. The figure is taken from [16].

It was observed in [16] that the $p_{\rm T}$ fluctuations are dominated by particles with relatively high $p_{\rm T}$. Figure 8 shows $F(p_{\rm T})$ as a function of upper $p_{\rm T}$ cut-off for the centrality corresponding to the maximal fluctuations. For a given $p_{\rm T}^{\rm max}$ only particles with $p_{\rm T} < p_{\rm T}^{\rm max}$ are taken into account. As seen, $F(p_{\rm T})$ grows fast with $p_{\rm T}^{\rm max}$ and consequently it was claimed [16] that the $p_{\rm T}$ fluctuations are due to jets or mini-jets. The claim, however, was questioned in [24] where it was argued that the data from Fig. 8 can be reproduced within a statistical model with multiple clusters or fireballs which move at some collective velocities, correlating the momenta of particles belonging to the same cluster. Thus, similarly to the situation at SPS, there is no unique interpretation of dynamical $p_{\rm T}$ fluctuations at RHIC.

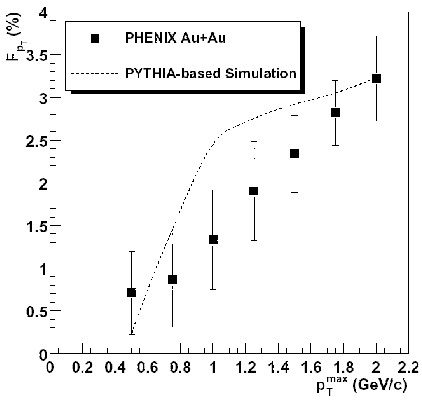

Fig. 8. $F(p_{\rm T})$ as a function of upper $p_{\rm T}$ cut-off for $N_{\rm part} \approx 150$ in Au–Au collisions at $\sqrt{s_{\rm NN}} = 200$ GeV. The figure is taken from [16].

7. Thermodynamic fluctuations

As mentioned in the Introduction, fluctuations in many body systems carry information about the system's state and its dynamics. Assuming that the strongly interacting matter produced in relativistic heavy-ion collisions is in thermodynamic equilibrium, it was suggested [26, 27] to measure the temperature fluctuations. Then, using the relation

$$\langle T^2 \rangle - \langle T \rangle^2 = \frac{\langle T \rangle^2}{C_V}\,, \tag{12}$$

which is discussed by Landau and Lifshitz [25], one can infer the system's heat capacity at fixed volume V and particle number N

$$C_V \equiv \left(\frac{\partial U}{\partial T}\right)_{V,N}, \tag{13}$$

where U is the system's energy. The relation (12), however, is actually very controversial [28,29] and its status is rather unclear. Not entering the details, I think that the relation (12) cannot be used, as long as the thermometer to measure the temperature fluctuations is not specified [30].

A similar idea [31] was to infer the compressibility

$$\kappa \equiv -\left(\frac{\partial p}{\partial V}\right)_{T,\langle N\rangle} , \tag{14}$$

where p is the pressure, from the multiplicity fluctuations due to the relation [25]

$$\langle N^2\rangle - \langle N\rangle^2 = \frac{T\langle N\rangle^2}{V^2\kappa} . \tag{15}$$

An experimental problem here is to measure the multiplicity fluctuations at fixed system's volume.

Only the third idea to study electric charge fluctuations in relativistic heavy-ion collisions appeared to be experimentally relevant. The fluctuations are related to the electric charge susceptibility [2] as

$$\langle Q^2\rangle - \langle Q\rangle^2 = TV\chi_Q , \tag{16}$$

with

$$\chi_Q \equiv -\left(\frac{\partial F}{\partial \mu_Q}\right)_{T,V} , \tag{17}$$

where F is the free energy and μ_Q is the chemical potential responsible for the electric charge conservation. Eqs. (16), (17) do not look very exciting at first glance but it was sharply observed [32, 33] that the susceptibility (17) is very different in the quark phase and in the hadron one.

To explain this statement, let me consider the classical ideal gas of particles of chargers $\pm q$ (measured in the units of elementary charge). The system's charge is then $Q = q(N_+ - N_-)$. We introduce $\delta Q \equiv Q - \langle Q\rangle$ and $\delta N_\pm \equiv N_\pm - \langle N_\pm\rangle$ and we compute the charge fluctuations as

$$\left\langle(\delta Q)^2\right\rangle = q^2\left\langle(\delta N_+ - \delta N_-)^2\right\rangle = q^2\Big(\left\langle(\delta N_+)^2\right\rangle + \left\langle\delta N_-)^2\right\rangle - 2\langle\delta N_+\delta N_-\rangle\Big) .$$

Since in the ideal classical gas $\langle(\delta N_\pm)^2\rangle = \langle N_\pm\rangle$ and $\langle\delta N_+\delta N_-\rangle = 0$, one finds

$$\frac{\left\langle(\delta Q)^2\right\rangle}{\langle N\rangle} = q^2 . \tag{18}$$

where $\langle N\rangle \equiv \langle N_+\rangle + \langle N_-\rangle$. As seen in Eq. (18), the charge fluctuation per particle equals the particle's charge squared.

One easily derives the formula analogous to Eq. (18) for the ideal classical gas of pions composed of π^+, π^-, π^0 and for the quark–gluon plasma being a mixture of ideal classical gases of quarks of different charges and of neutral gluons. Using the system's entropy S instead of the total particle multiplicity $\langle N \rangle$, one finds [2]

$$\frac{\langle (\delta Q)^2 \rangle}{S} = \begin{cases} \frac{1}{6} & \text{for pions}\,, \\ \frac{1}{24} & \text{for QGP}\,. \end{cases} \tag{19}$$

It was argued in [32, 33] that the charge fluctuations generated in the quark phase are frozen due the system's fast hydrodynamic expansion and that the entropy, which is mostly produced at the very early, preequilibrium stage of the collision, is approximately conserved during the hydrodynamic evolution. Then, a measurement of the ratio (19) should clearly show whether the quark–gluon plasma is produced at the early stage of relativistic heavy-ion collisions.

Soon later the electric charge fluctuation were measured experimentally. Figs. 9 and 10 show the results obtained at SPS by NA49 Collaboration [34] using the measure Φ defined by Eq. (5). $\langle N_{\rm ch} \rangle_{\rm tot}$ and $\langle N_{\rm ch} \rangle$ are the average charge particle multiplicities in, respectively, the full (4π) acceptance and in a given phase-space domain under study. As seen, the results, which are essentially independent of the collision energy, follow the trend dictated by the global charge conservation (GCC) corresponding to

$$\Phi_q^{\rm GCC} = \sqrt{1 - \frac{\langle N_{\rm ch} \rangle}{\langle N_{\rm ch} \rangle_{\rm tot}}} - 1\,. \tag{20}$$

The formula (20) derived in [35] is actually approximate as it is derived under the assumption that the total system's charge Z vanishes. It is, however, a reasonable approximation of the exact formula derived in [36] when $Z \ll \langle N_{\rm ch} \rangle_{\rm tot},$.

Figure 10 shows the electric charge fluctuations when the effect of the global charge conservation is subtracted that is there is presented $\Delta\Phi_q \equiv \Phi_q - \Phi_q^{\rm GCC}$. Figure 10 also shows the levels of charge fluctuations in the quark–gluon plasma and in the hadronized system, both computed in a rather simplified model. As seen, the observed fluctuations agree very well with the hadron gas prediction.

The electric charge fluctuations were measured at RHIC by PHENIX [37] and STAR [38, 39] Collaborations. The results shown in Fig. 11, which is taken from [39], are rather similar to those obtained at SPS. However, the STAR Collaboration used the measure $\nu_{+-}^{\rm dyn}$ to quantify the electric charge

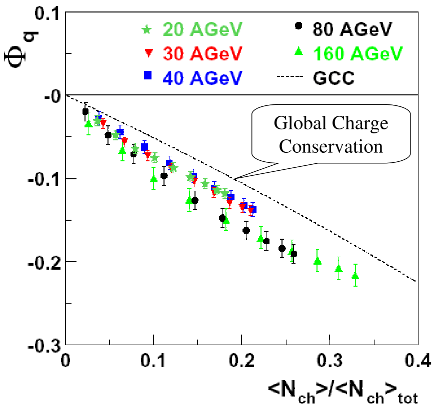

Fig. 9. Electric charge fluctuations quantified by Φ_q as a function of relative charge multiplicity in central Pb–Pb collisions at SPS for several collision energies. The figure is taken from [34].

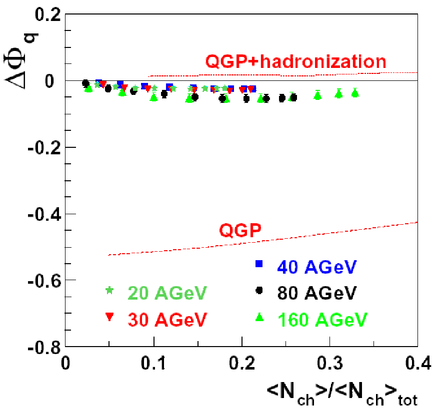

Fig. 10. Electric charge fluctuations quantified by $\Delta\Phi_q \equiv \Phi_q - \Phi_q^{\rm GCC}$ as a function of relative charge multiplicity in central Pb–Pb collisions at SPS for several collision energies. The figure is taken from [34].

fluctuations. It is defined as

$$\nu_{+-}^{\rm dyn} \equiv \frac{\langle N_+(N_+-1)\rangle}{\langle N_+\rangle^2} + \frac{\langle N_-(N_--1)\rangle}{\langle N_-\rangle^2} - 2\frac{\langle N_+N_-\rangle}{\langle N_+\rangle\langle N_-\rangle} \,. \tag{21}$$

$\nu_{+-}^{\rm dyn}$ is sensitive only to the dynamic fluctuations in this sense that it vanishes when the fluctuations of both N_+ and N_- are Poissonian.

As seen in Fig. 11, the observed fluctuations are not only bigger than those in QGP but they are even bigger than those in the hadron resonance gas. Although we have good reason to claim that the quark–gluon plasma is produced at the early stage of relativistic heavy-ion collisions at RHIC, the final state charge fluctuations do not signal the presence of the QGP. Most probably the fluctuations generated at the plasma phase are simply washed out during the subsequent system's evolution. The fact that the observed charge fluctuations are bigger than those in the hadron resonance gas is presumably caused by a relatively small acceptance of the measurement. When a significant fraction of particles originate from neutral resonances, which decay into one positive and one negative particles, the charge fluctuations are reduced, when compared to the Poissonian fluctuations, if both particles from the decay are observed [35]. When the experimental acceptance is so small that typically only one particle from a resonance decay is registered, the electric charge fluctuations remain Poissonian.

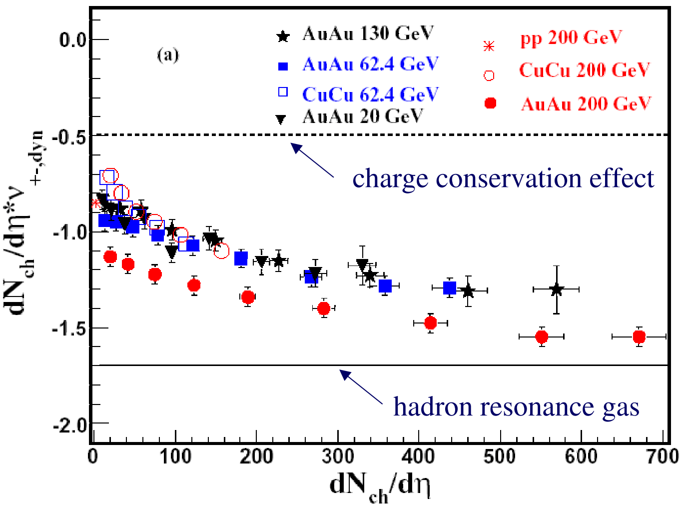

Fig. 11. Electric charge fluctuations quantified by $\nu_{+-}^{\rm dyn}$ as a function of pseudorapidity density of charged particles in nucleus–nucleus collisions at RHIC collision energies. The vertical axis shows $\nu_{+-}^{\rm dyn}$ multiplied by the pseudorapidity density of charged particles. The figure is taken from [39].

8. Balance functions

In the previous section I discussed bulk fluctuations of electric charge which at the end appeared to be not very informative. Here I am going to present a very interesting idea [40,41] to measure correlations of the electric charges in rapidity by means of the so-called balance functions defined as

$$B(\Delta y) \equiv \frac{1}{2}\left[\frac{\langle N_{+-}(\Delta y)\rangle - \langle N_{--}(\Delta y)\rangle}{\langle N_{-}(\Delta y)\rangle} + \frac{\langle N_{-+}(\Delta y)\rangle - \langle N_{++}(\Delta y)\rangle}{\langle N_{+}(\Delta y)\rangle}\right], \quad (22)$$

where $\langle N_{\pm}(\Delta y)\rangle$ and $\langle N_{\pm\pm}(\Delta y)\rangle$ are, respectively, the average number of positive or negative particles and the average number of pairs of particles of given charges within the rapidity (or pseudorapidity) interval Δy ($\Delta\eta$). The balance functions were argued [40, 42] be sensitive to a hadronization mechanism. The width of the balance functions was expected to be bigger, when the hadronization proceeds via the break-up of strings as in p–p collisions, than when the quark–gluon plasma hadronizes due to the coalescence of constituent quarks.

The balance functions were measured in Au+Au collisions at RHIC [43] and in Pb–Pb collisions at SPS [44], see Fig. 12 and 13. The balance functions for peripheral collisions appeared to have widths consistent with model predictions based on a superposition of nucleon–nucleon scattering. Widths

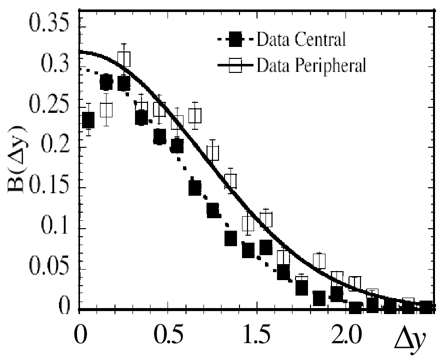

Fig. 12. The balance functions in central and peripheral Au–Au collisions $\sqrt{s_{\rm NN}} =$ 130 GeV. The figure is taken from [43].

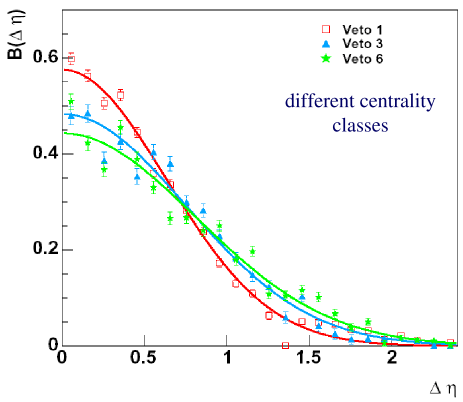

Fig. 13. The balance functions in Pb–Pb collisions at different centralities at 158 A GeV. The centrality class 'Veto 1' corresponds to the most central collisions. The figure is taken from [44].

in central collisions were smaller, consistent with trends predicted by models incorporating late hadronization due to the coalescence mechanism. Unfortunately, the interpretation appeared to be not unique as the balance functions were shown to be influenced by various factors [45–47]. In particular, it was observed that the variation of the amount of transverse flow with collision centrality can reproduce [47] the experimentally observed narrowing of the balance functions for central collisions.

9. Multiplicity fluctuations

As discussed in Sec. 3, the multiplicity measurements like that one presented in Fig. 2 are not very useful, as the results crucially depend on the collision centrality. The situation is changed if the centrality condition does not result from specific features of a detector used in the measurement but if the centrality condition corresponds to a well defined physical criterion. Such measurements were performed by the NA49 Collaboration [48] with the help of zero degree calorimeter which allowed one to determine the number of participating nucleons from a projectile ($N_{\rm part}^{\rm projectile}$) in a given nucleus–nucleus collision. Figure 14 shows the scaled variance ($\langle (N - \langle N \rangle)^2 \rangle / \langle N \rangle$) as a function of $N_{\rm part}^{\rm projectile}$ in p–p and Pb–Pb collisions at 158 A GeV [48]. We observe a non-monotonic behavior of $\langle (N - \langle N \rangle)^2 \rangle / \langle N \rangle$ which contradicts commonly applied models. In the Wounded Nucleon Model [8], where produced particles come from wounded nucleons, which are assumed to be independent from each other, the scale variance is exactly independent of $N_{\rm part}^{\rm projectile}$. As seen in Fig. 14, the transport models HIJING [9], VENUS [10], UrQMD [11] or HSD [12] predict the approximate independence. It should be noted here that although the scaled variance is a non-monotonic function of $N_{\rm part}^{\rm projectile}$, the average multiplicity is simply proportional to $N_{\rm part}^{\rm projectile}$ [48] in agreement with the models mentioned above. Although there were several theoretical attempts [49–52] to explain the data shown in Fig. 14, in my opinion, there is no reliable explanation.

The multiplicity distribution at the most central collisions reveals an interesting feature. As shown in Fig. 15 taken form [53] it is narrower not only than the Poisson distribution but it is narrower than the multiplicity distribution obtained in the statistical model [54] which uses the Canonical Ensemble where the electric charge is exactly conserved. As seen in Fig. 16, this feature persists in a broad range of collision energies. Figure 16 also shows that within statistical models one has to refer to a microcanonical ensemble to reproduce the scaled variance of multiplicity distribution.

The multiplicity distributions discussed here appear to be associated with the transverse momentum fluctuations discussed in Sec. 6. As seen in the definition of the measure Φ (5), it depends on the multiplicity distri-

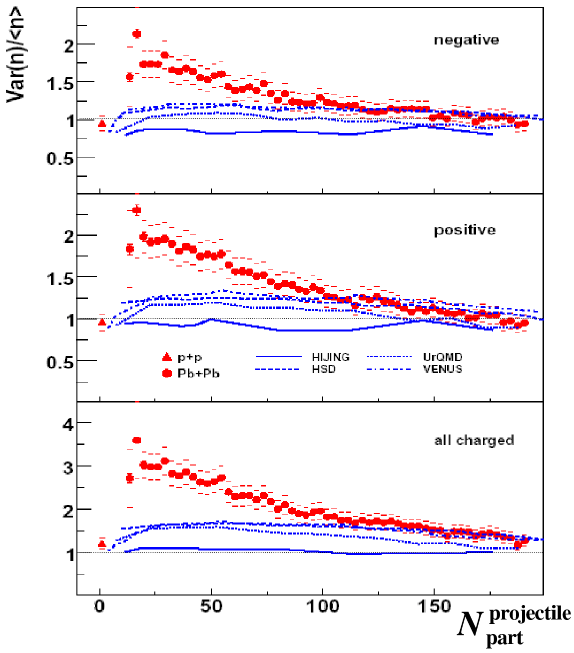

Fig. 14. The scaled variance of multiplicity distribution of negative (upper panel), positive (middle panel) and charged (lower panel) particles as a function of number of projectile participants in nucleus–nucleus collisions at 158 A GeV. The predictions of HIJING, VENUS, UrQMD and HSD models are also shown. The figure is taken from [48].

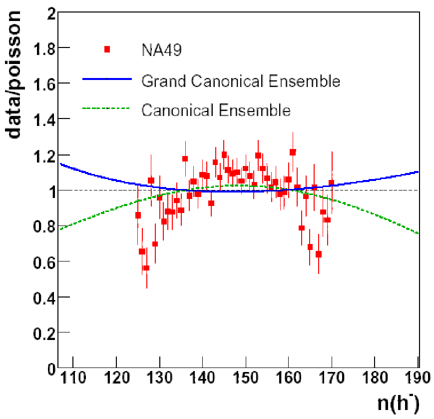

Fig. 15. The multiplicity distribution of negative charge particles produced in the most central Pb–Pb collisions at 158 A GeV. The distribution is divided by the Poisson distribution of the same mean. The predictions of statistical models based on the Grand Canonical and Canonical Ensembles are also shown. The figure is taken from [53].

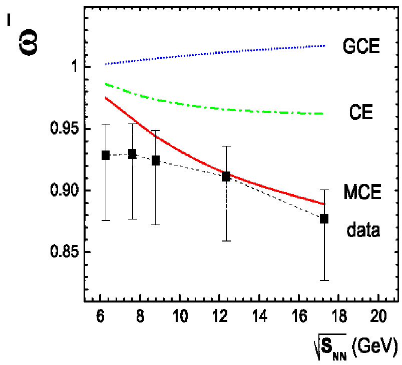

Fig. 16. The scaled variance of multiplicity distribution of negative particles produced in the most central Pb–Pb collisions as a function of collision energy. The predictions of statistical models based on the Grand Canonical, Canonical and Microcanonical Ensembles are also shown. The figure is taken from [54].

bution. It was shown in [22] that the correlation of the event's transverse momentum and multiplicity, which is observed in p–p collisions [21], combined with the non-monotonic scaled variance of multiplicity distribution shown in Fig. 14 approximately reproduces the $p_{\rm T}$ fluctuations shown Fig. 4. Therefore, the similarity of Figs. 4, 14 is far from not superficial.

10. Elliptic flow fluctuations

The elliptic flow is caused by an azimuthally asymmetric shape of the initial interaction zone of colliding nuclei. Consequently, it is mostly generated in the collision early stage. Fluctuations of the elliptic flow were argued to carry information on very early stages of relativistic heavy-ion collisions [55, 56]. Large fluctuations of the elliptic flow were indeed observed at RHIC by PHOBOS [57] and STAR [58] Collaborations. However, STAR Collaboration claimed later on [59] that the magnitude of the fluctuations should be taken only as an upper limit due to the difficulties to disentangle the elliptic flow fluctuations and the contributions which are not correlated with the reaction plane. PHOBOS Collaboration has not retracted the data [57]. The whole problem is discussed in detail in the very recent review [60].

As seen in Fig. 17, the relative v_2 fluctuations measured by PHOBOS Collaboration [57] are as large as about 40%. It appears, however, that the effect is dominated not by the dynamics but by simple geometrical fluctuations of the eccentricity of the interaction zone as suggested in [61]. Since the positions of nucleon–nucleon interactions fluctuate within the overlap region of the colliding nuclei as illustrated in Fig. 18 taken from [62], the eccentricity of the region fluctuates as well. Since the elliptic flow is proportional to the eccentricity, the relative eccentricity fluctuations directly contribute to the relative elliptic flow fluctuations. The calculations of the eccentricity fluctuations reproduce well the experimentally observed elliptic flow fluctuations, see *e.g.* [62]. Therefore, the hydrodynamic evolution of the system, when the elliptic flow is generated, seems to be fully deterministic. The result is rather paradoxical if one remembers that the elliptic flow is mostly generated at a very early stage of the collision when the produced matter is presumably not in a complete equilibrium yet.

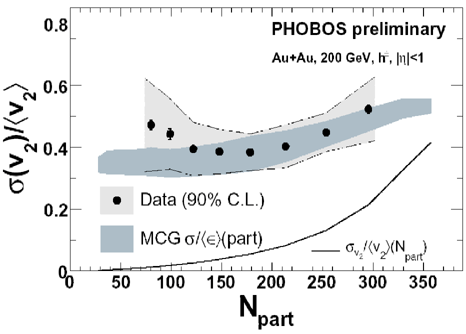

Fig. 17. The relative fluctuations of the elliptic flow in Au–Au collisions at $\sqrt{s_{\mathrm{NN}}} =$ 200 GeV. The figure is taken from [57].

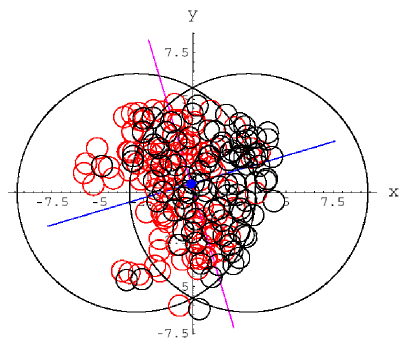

Fig. 18. Positions of wounded nucleons in the plane transverse to the beam in the Au–Au collision. The figure is taken from [62].

11. Conclusions and outlook

A big volume of experimental data on event-by-event fluctuations in relativistic heavy-ion collisions has been collected for last fifteen years. Some results are indeed very interesting but the observed fluctuations are usually dominated by statistical noise as convincingly illustrated by similarity of mixed and real events. Theoretical expectations of large fluctuations cased by, say, phase transitions appeared to be far too optimistic but measuring of the fluctuations has also appeared rather difficult.

When single particle distributions are measured a detector inefficiency is not a serious obstacle. A number of undetected particles should be estimated and the single particle distribution is then easily corrected. In the case of correlation measurements, the effect of lost particles on the measured correlation depends on how the lost particles are correlated with the detected ones. Since the correlation is *a priori* not known, it is unclear how the observed correlation should be corrected. For this reason, the correlation measurements were usually performed in rather small acceptances where the detector efficiency is almost perfect. Then, the observed correlation signal does not need a correction for lost particles. However, dynamical correlations are usually strongly diluted due to a small acceptance. As an example, let me consider a multiplicity distribution. If we detect only a small fraction p of all particles, the observed multiplicity tends to the Poisson distribution when $p \to 0$. Consequently, we observe the Poisson distribution in a small acceptance independently of the actual distribution. I note that currently no more than 20% but typically only a few percent of all produced particles are used in event-by-event studies.

Another problem of the current experiments is that the actual colliding system is not well known as an averaging over a centrality interval is performed. Such an averaging dilutes a potential signal, as most of characteristics of heavy-ion collisions strongly depends on centrality. Sometimes the centrality is estimated using produced particles which are analyzed. Then, the effect of autocorrelation has to be additionally removed from the data.

The analysis of multiplicity clearly shows how important is a good determination of centrality. The multiplicity measurement presented in Fig. 2 badly depends on experimental condition and thus is not very useful. When the collision centrality is so precisely measured that the number of participating nucleons from a projectile is known, the multiplicity distribution appeared to conceal very interesting features displayed in Figs. 14, 15.

As the observed dynamical fluctuations are usually small, it is difficult to extract physically interesting information, it is even more difficult to workout a unique interpretation. New theoretical ideas and reliable models are certainly needed but what the event-by-event physics really requires is, in my opinion, a new generation of experiments which will fulfill two important conditions: *(i)* the acceptance is a sizeable fraction of 4π, *(ii)* the collision centrality is measured up to single nucleons participating in a collision. The future NA61/SHINE program at SPS is hoped to satisfy the requirements [63].

This work was partially supported by the Polish Ministry of Science and Higher Education under grant No N202 3956 33.

REFERENCES

[1] H. Heiselberg, *Phys. Rep.* **351**, 161 (2001).

[2] S. Jeon, V. Koch, in *Quark Gluon Plasma 3*, eds. R.C. Hwa, X.-N. Wang, Scientific, Singapore 2004.

[3] R. Stock, in *Proceedings of NATO Advanced Study Workshop on Hot Hadronic Matter: Theory and Experiment*, Divonne-les-Bains, France, June 27–July 1, 1994, eds. J. Letessier, H.H. Gutbrod, J. Rafelski, Plenum Press, New York 1995.

[4] H. Appelshauser *et al.* [NA49 Collaboration], *Phys. Lett.* **B459**, 679 (1999).

[5] M.M. Aggarwal *et al.* [WA98 Collaboration], *Phys. Rev.* **C65**, 054912 (2002).

[6] K. Adcox *et al.* [PHENIX Collaboration], *Phys. Rev.* **C66**, 024901 (2002).

[7] M. Gaździcki, St. Mrówczyński, *Z. Phys.* **C54**, 127 (1992).

[8] A. Białas, M. Błeszynski, W. Czyż, *Nucl. Phys.* **B111**, 461 (1976).

[9] X.N. Wang, M. Gyulassy, *Phys. Rev.* **D44**, 3501 (1991).

[10] K. Werner, *Phys. Rep.* **232**, 87 (1993).

[11] S.A. Bass *et al.*, *Prog. Part. Nucl. Phys.* **41**, 255 (1998).

[12] W. Cassing, E.L. Bratkovskaya, *Phys. Rep.* **308**, 65 (1999).

[13] S.A. Voloshin, V. Koch, H.G. Ritter, *Phys. Rev.* **C60**, 024901 (1999).

[14] T.A. Trainor, `arXiv:hep-ph/0001148`.

[15] D. Adamova *et al.* [CERES Collaboration], *Nucl. Phys.* **A727**, 97 (2003).

[16] S.S. Adler *et al.* [PHENIX Collaboration], *Phys. Rev. Lett.* **93**, 092301 (2004).

[17] T. Anticic *et al.* [NA49 Collaboration], *Phys. Rev.* **C70**, 034902 (2004).

[18] A. Białas, M. Gaździcki, *Phys. Lett.* **B252**, 483 (1990).

[19] K. Grebieszkow *et al.* [NA49 Collaboration], *PoS* **CPOD07**, 022 (2007).

[20] D. Adamova *et al.* [CERES Collaboration], *Nucl. Phys.* **A811**, 179 (2008).

[21] T. Kafka *et al.*, *Phys. Rev.* **D16**, 1261 (1977).

[22] St. Mrówczyński, M. Rybczyński, Z. Włodarczyk, *Phys. Rev.* **C70**, 054906 (2004).

[23] J. Adams *et al.* [STAR Collaboration], *Phys. Rev.* **C71**, 064906 (2005).

[24] W. Broniowski, P. Bożek, W. Florkowski, B. Hiller, *PoS* **CFRNC2006**, 020 (2006).

[25] L.D. Landau, E.M. Lifshitz, *Statistical Physics*, Pergamon Press, Oxford 1980.

[26] L. Stodolsky, *Phys. Rev. Lett.* **75**, 1044 (1995).

[27] E.V. Shuryak, *Phys. Lett.* **B423**, 9 (1998).

[28] C. Kittel, *Phys. Today* **41**, 93 (1988).

[29] B. Mandelbrot, *Phys. Today* **42**, 71 (1988).

[30] M.A. Stephanov, K. Rajagopal, E.V. Shuryak, *Phys. Rev.* **D60**, 114028 (1999).

[31] St. Mrówczyński, *Phys. Lett.* **B430**, 9 (1998).

[32] S. Jeon, V. Koch, *Phys. Rev. Lett.* **85**, 2076 (2000).

[33] M. Asakawa, U.W. Heinz, B. Muller, *Phys. Rev. Lett.* **85**, 2072 (2000).

[34] C. Alt *et al.* [NA49 Collaboration], *Phys. Rev.* **C70**, 064903 (2004).

[35] J. Zaranek, *Phys. Rev.* **C66**, 024905 (2002).

[36] St. Mrówczyński, *Phys. Rev.* **C66**, 024904 (2002).

[37] K. Adcox *et al.* [PHENIX Collaboration], *Phys. Rev. Lett.* **89**, 082301 (2002).

[38] J. Adams *et al.* [STAR Collaboration], *Phys. Rev.* **C68**, 044905 (2003).

[39] B.I. Abelev *et al.* [STAR Collaboration], `arXiv:0807.3269 [nucl-ex]`.

[40] S.A. Bass, P. Danielewicz, S. Pratt, *Phys. Rev. Lett.* **85**, 2689 (2000).

[41] S. Jeon, S. Pratt, *Phys. Rev.* **C65**, 044902 (2002).

[42] A. Białas, *Phys. Lett.* **B579**, 31 (2004).

[43] J. Adams *et al.* [STAR Collaboration], *Phys. Rev. Lett.* **90**, 172301 (2003).

[44] C. Alt *et al.* [NA49 Collaboration], *Phys. Rev.* **C71**, 034903 (2005).

[45] S. Pratt, S. Cheng, *Phys. Rev.* **C68**, 014907 (2003).

[46] P. Bożek, W. Broniowski, W. Florkowski, *Acta Phys. Hung.* **A22**, 149 (2005).

[47] S. Cheng *et al.*, *Phys. Rev.* **C69**, 054906 (2004).

[48] C. Alt *et al.* [NA49 Collaboration], *Phys. Rev.* **C75**, 064904 (2007).

[49] M. Rybczyński, Z. Włodarczyk, *J. Phys. Conf. Ser.* **5**, 238 (2005).

[50] M. Gaździcki, M.I. Gorenstein, *Phys. Lett.* **B640**, 155 (2006).

[51] L. Cunqueiro, E.G. Ferreiro, F. del Moral, C. Pajares, *Phys. Rev.* **C72**, 024907 (2005).

[52] P. Brogueira, J. Dias de Deus, *Phys. Rev.* **C72**, 044903 (2005).

[53] C. Alt *et al.* [NA49 Collaboration], `arXiv:0712.3216 [nucl-ex]`.

[54] V.V. Begun, M. Gaździcki, M.I. Gorenstein, M. Hauer, V.P. Konchakovski, B. Lungwitz, *Phys. Rev.* **C76**, 024902 (2007).

[55] St. Mrówczyński, E.V. Shuryak, *Acta Phys. Pol. B* **34**, 4241 (2003).

[56] St. Mrówczyński, *J. Phys. Conf. Ser.* **27**, 204 (2005).

[57] B. Alver *et al.* [PHOBOS Collaboration], *J. Phys. G* **34**, S907 (2007).

[58] P. Sorensen [STAR Collaboration], *J. Phys. G* **34**, S897 (2007).

[59] P. Sorensen [STAR Collaboration], `arXiv:nucl-ex/0612021`.

[60] S.A. Voloshin, A. M. Poskanzer, R. Snellings, `arXiv:0809.2949 [nucl-ex]`.

[61] M. Miller, R. Snellings, `arXiv:nucl-ex/0312008`.

[62] W. Broniowski, P. Bożek, M. Rybczyński, *Phys. Rev.* **C76**, 054905 (2007).

[63] M. Gaździcki [NA61/SHINE Collaboration], `arXiv:0812.4415 [nucl-ex]`.